ACS APPLIED MATERIALS & INTERFACES

Subscriber access provided by UNIVERSITY OF LEEDS

Article

Carbonized leaf membrane with anisotropic surfaces for sodium ion battery

Hongbian Li, Fei Shen, Wei Luo, Jiaqi Dai, Xiaogang Han, Yanan Chen, Yonggang Yao, Kun Fu, Hongli Zhu, Emily Michelle Hitz, and Liangbing Hu

ACS Appl. Mater. Interfaces, **Just Accepted Manuscript** • DOI: 10.1021/acsami.5b10875 • Publication Date (Web): 04 Jan 2016

Downloaded from http://pubs.acs.org on January 9, 2016

Just Accepted

"Just Accepted" manuscripts have been peer-reviewed and accepted for publication. They are posted online prior to technical editing, formatting for publication and author proofing. The American Chemical Society provides "Just Accepted" as a free service to the research community to expedite the dissemination of scientific material as soon as possible after acceptance. "Just Accepted" manuscripts appear in full in PDF format accompanied by an HTML abstract. "Just Accepted" manuscripts have been fully peer reviewed, but should not be considered the official version of record. They are accessible to all readers and citable by the Digital Object Identifier (DOI®). "Just Accepted" is an optional service offered to authors. Therefore, the "Just Accepted" Web site may not include all articles that will be published in the journal. After a manuscript is technically edited and formatted, it will be removed from the "Just Accepted" Web site and published as an ASAP article. Note that technical editing may introduce minor changes to the manuscript text and/or graphics which could affect content, and all legal disclaimers and ethical guidelines that apply to the journal pertain. ACS cannot be held responsible for errors or consequences arising from the use of information contained in these "Just Accepted" manuscripts.

ACS Publications

ACS Applied Materials & Interfaces is published by the American Chemical Society. 1155 Sixteenth Street N.W., Washington, DC 20036

Published by American Chemical Society. Copyright © American Chemical Society. However, no copyright claim is made to original U.S. Government works, or works produced by employees of any Commonwealth realm Crown government in the course of their duties.

Carbonized Leaf Membrane with Anisotropic Surfaces for Sodium Ion Battery

Hongbian Li,[1,2†] Fei Shen,[1†] Wei Luo,[1] Jiaqi Dai,[1] Xiaogang Han,[1] Yanan Chen,[1] Yonggang Yao,[1] Hongli Zhu,[1] Kun Fu,[1] Emily Hitz,[1] Liangbing Hu*[1]

[1]Department of Materials Science and Engineering, University of Maryland, College Park, MD 20742, USA
[2]National Center for Nanoscience and Technology, 11, Beiyitiao, Zhonguancun, Beijing, 100190, China
*Email: binghu@umd.edu
[†]H. Li and F. Shen contribute equally to this work.

ABSTRACT

A simple one-step thermal pyrolysis route has been developed to prepare carbon membrane from a natural leaf. The carbonized leaf membrane possesses anisotropic surfaces and internal hierarchical porosity, exhibiting a high specific capacity of 360 mAh/g and a high initial Coulombic efficiency of 74.8% as a binder-free, current collector-free anode for rechargeable sodium ion batteries. Moreover, large area carbon membranes with low contact resistance are fabricated by simply stacking and carbonizing leaves, a promising strategy toward large-scale sodium ion battery developments.

KEYWORDS

Leaf; Carbon membrane; Freestanding; Sodium ion battery; Initial Coulombic efficiency

INTRODUCTION

With the abundance of sodium source, sodium ion batteries (SIBs) are considered to be a promising alternative for lithium ion batteries (LIBs) particularly for grid-scale energy storage.[1-8] To achieve affordable and high efficient SIBs, the development of high performance and cost-effective electrode materials is crucial. According to the well-developed LIB knowledge, great progress has been made in developing suitable SIB cathodes.[9-14] However, the challenge for SIBs is the anode, since graphite, which is the standard LIB anode, is very limited in its ability to store sodium ions due to the their larger ionic size.[15] Although exfoliating graphite and further functionalizing them (like doping or combining with other active materials) can greatly increase their performance in sodium ion storage,[16-20] the exfoliating process is time-costive and result much pollution. Therefore, a low-cost and easily fabricated pure carbon electrode needs to be developed.

Hard carbon, which is formed by short-range turbo static structures, has shown high capacity as an anode for SIBs in recent years.[21-24] Biomass, which is abundant and renewable, provides a low-cost and environmental friendly hard carbon precursor for SIB anodes.[25-27] There are several mechanisms for the storage of sodium ion in hard carbon anode, for example, intercalation between short-range graphene layers[28, 29], nanopore filling [30,31] and chemisorption on surface heteroatoms[32] or structure defects[33]. In hard carbon, there are a lot of voids between the short-range turbo layers, which can provide many cavities for storing sodium ions, leading to a higher capacity compared to graphite.[34] Several biomass, such as lignin[35] sucrose,[36] peat moss,[37] banana peels,[38] cellulose nanofiber,[39] silk[40,41] and melo peels[42] have been used as carbon precursors, and their derived carbons have exhibited great performance as SIB anodes. However, these carbon powder need to be mixed with carbon black and

polymer binders to form the electrodes using slurry coating method, which requires extra steps for the battery fabrication and also results in an additional weight. To avoid the extra mixing process, simplify the battery fabrication process and increase the energy density of the full battery, a freestanding carbon electrode is highly desirable.[43-45] Another problem of hard carbon anode is the low initial Coulombic efficiency (<50%) caused by the formation of solid electrolyte interface (SEI) and irreversibly Na^+ trap in the graphene layers and defect sites,[29] which result in an irreversible loss of sodium ions and a waste of cathode material in the full battery. Therefore, rational design of the pore structure in the carbon anodes for limited SEI formation and high capacity is crucial for high-performance SIBs.

Natural leaf, which is one of the most abundant biomass sources on Earth, with the main composition of cellulose, hemicellulose and lignin,[46] can be carbonized by thermal pyrolysis. As the anode for SIB, carbon derived leaf over performs others by three points: (1) Leaf has anisotropic surfaces, in which stomata on the back surface (facing the soil) provide channels for the electrolyte to enter into the overlapping carbon nanosheets inside the carbonized leaf, and the non-porous upper surface (facing the Sun) can work as a dense current collector, enabling the carbonized leaf to be a binder/current collector-free anode for SIBs. (2) The pores in carbonized leaf are in the range of micrometers, resulting in a low surface area and limited SEI formation for higher initial Coulombic efficiency. (3) The carbon membrane from leaf is freestanding with a thickness around 50 to 200 μm,[47-49] which is suitable for battery electrode application and avoids further mixing with other additives during battery fabrication process. Together with these properties, carbonized leaf could provide a high-performance and low-cost anode material for the scalable fabrication of SIBs.

Here we prepared a freestanding carbon membrane from leaf, and for the first time

used it as a binder/current collector- free anode for SIBs. The carbon membrane is highly conductive with a conductivity of 1259 $S.m^{-1}$. Hierarchical pores inherited from the leaf provide special channels for the electrolyte to access to the carbon nanosheets inside. Unlike nanoporous carbon powder and less-porous carbon bulk electrode, most of the pores in the leaf-based membrane are macropores, which are surrounded by amounts of nanosheets, thereby, achieving a high capacity and high initial Coulombic efficiency simultaneously.

EXPERIMENTAL SECTION

Materials synthesis

Dry maple leaf was collected on campus and used without further treatment. The leaf was put into a tube furnace and carbonized at 1000 °C for 1 h under Ar flow with a ramping rate of 10 °C/min. To avoid curling, the leaf was fastened between graphite slides during the carbonization process. After the reaction, the carbonized leaf was immersed in 3.0 M HCl for 6 h to remove the inorganic impurities.

Characterization of the materials

The morphology of the carbonized leaf was observed with Hitachi SU-70 analytical scanning electron microscope (SEM) and a JEM 2100 FETEM transmission electron microscope (TEM). The structure of the carbonized leaf was measured with D8 Advance X-Ray Diffraction (XRD) System and Horiba Yvon LabRam ARAMIS confocal Raman microscope with a heliumneon 10 mW laser excitation source (632.8 Raman). Brunauer-Emmett-Teller (BET) analysis for nitrogen adsorption and desorption isotherms were performed on a Tristar II 3020 analyzer.

Electrochemical measurements

Electrochemical properties of the carbonized leaf were determined using 2032 coin cells with Na plates as the counter/reference electrodes, and 1.0 M $NaClO_4$ in ethylene carbonate (EC)/ diethyl carbonate (DEC) as the electrolyte. The cells were tested by Arbin BT2000 battery tester.

RESULTS AND DISCUSSION

Figure 1a shows the typical structure of a natural leaf with anisotropic surfaces, where the upper surface is flat, dense and made up of many interconnected domains to prevent fast water evaporation (Figure 1b). In contrast to the upper surface, the back surface features many uniformly-distributed stomata for gas exchange and water evaporation during transpiration (Figure 1c). The inner section of the leaf is highly porous with many cells to form the hollow tube structures. Figure 1d shows a cross-section of the leaf, revealing the porous structure of its interior. Tubes beneath the upper layer arrange vertically to form the palisade layer, which provides more chloroplasts for photosynthesis. Under the well-aligned tube array is the sponge layer, where the tubes loosely and randomly distribute to leave enough air space for the exchange of oxygen and carbon dioxide during leaf respiration and photosynthesis.[50-53]

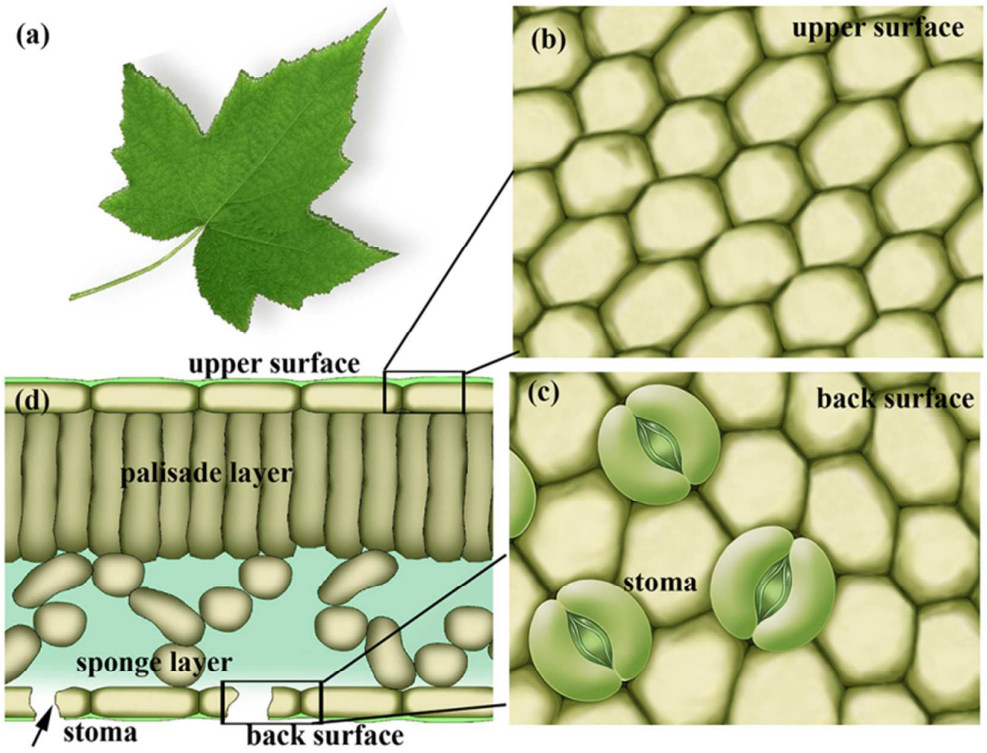

Figure 1. (a) The schematic illustration of a leaf, and its (b) upper surface; (c) back surface and (d) cross-section part.

After carbonization at 1000 °C under Argon, as shown in Figure 2a, the dried natural leaf turns black, indicating successful transformation into carbon. The carbonized leaf membrane maintains the shape of the original leaf, indicating good mechanical strength as a freestanding electrode for battery applications. In addition, the carbonized leaf membrane inherits the inner porous structure of the original leaf, as shown in the SEM image of the cross-section part in Figure 2b. One can see the porous back surface and the dense upper surface clearly. The total thickness of the carbonized leaf is about 60 μm, with the upper surface and the back surface 5 μm and 2 μm thick, respectively. The inner side of the carbonized leaf is highly porous with many nanosheets overlapped with each other, similar to freeze-dried graphene foam.[54]

This unique porous structure facilitates the transport of the electrolyte (blue arrows) with least resistance to the carbon sheets inside the carbonized leaf, entering through the porous back surface to the loosely arranged sponge layer (about 20 μm) that has many voids located near the back surface, and finally to well-aligned palisade layer (about 30μm). Electrons travel along the conductive carbon sheet in the carbonized leaf and then are collected by the dense upper surface layer (red arrow). When zoomed in, it can be found that the thickness of the carbon sheet from the cell wall is in the range of 50-100 nm (Figure 2c), which allows for a short diffusion length for the sodium ions and leads to a high capacity. Due to the existence of inorganic elements in the natural leaves, there are some inorganic particles formed on the surface of the carbonized leaf (Figure S1-S3 in the supporting information). X-ray diffraction (XRD) patterns (Figure S4) indicate these particles are mainly $Ca(OH)_2$,[55] which may result from the hydrolysis of CaO when the carbonized leaf is exposed to the moisture in air. These inorganic particles are easily removed by immersing the carbonized leaf in 3 M HCl for 6 h. As shown in Figure 2d, the clean back surface exhibits a large number of grinning-mouth like open macro pores (stomata). These macro-sized pores are well-connected to those inside the leaf (Figure S5), facilitating the fast intrusion of the electrolyte into the inner pores of the carbonized leaf (blue arrows). For the upper surface, no pores are observed but grains from quadrilateral to pentagon and then hexagon appear (Figure 2e). These grains assemble like bricks into a flat dense surface, which is used as the current collector during electrochemical reactions (red arrow). The TEM image in Figure 2f gives further the insight to the microstructure of the carbonized leaf, where a typical morphology of amorphous carbon, having short-range aligned lattice and some voids were found. The measured lattice distance for the ordered region is 0.36 nm, slightly larger than that of graphite

(0.34 nm).

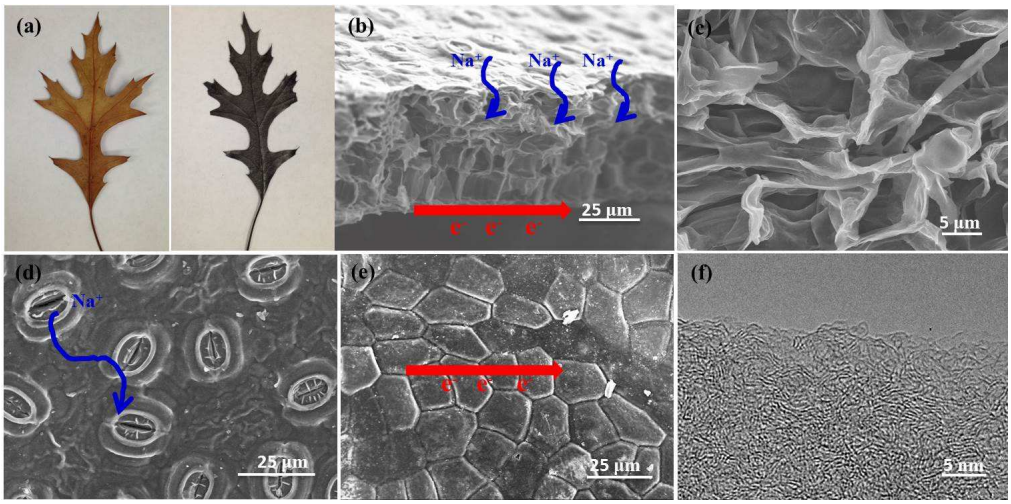

Figure 2. (a) Digital pictures of a dried leaf before and after carbonization. (b) A SEM image of the cross-section of the carbonized leaf. (c) The magnified SEM image of the carbon nanosheet in the sponge layer. (d) A SEM images of the stomata distributed uniformly on the back surface. (e) A SEM image of the brick-like grains on the upper surface. (f) A HRTEM image of the carbonized leaf.

To further study the structure of the carbonized leaf, XRD pattern and Raman spectra were collected and the results are shown in Figure 3. The XRD pattern in Figure 3a shows two broad diffraction peaks at 22.9° and 43.2° for (002) and (101) planes of the typical amorphous carbon. Raman spectrum of the carbonized leaf in Figure 3b exhibits two peaks for the D-band at 1346 cm^{-1} and G band at 1598 cm^{-1}, with an intensity ratio I_D/I_G of 1.14. This further confirms the amorphous nature of the carbonized leaf, which can be used as anode for SIBs. The N_2 adsorption-desorption isotherm in Figure 3c demonstrates the pore structure of the carbonized leaf, which is a typical II isotherm corresponding to the adsorption of the macroporous materials.

The calculated surface area is 161 m^2/g. This low surface area could induce limited SEI formation and thus a high initial Coulombic efficiency. The pore size distribution curve in Figure 3d shows limited amounts of nanopores. Most of the pores are macropores from the original leaf, which agrees well with the result of a low surface area.

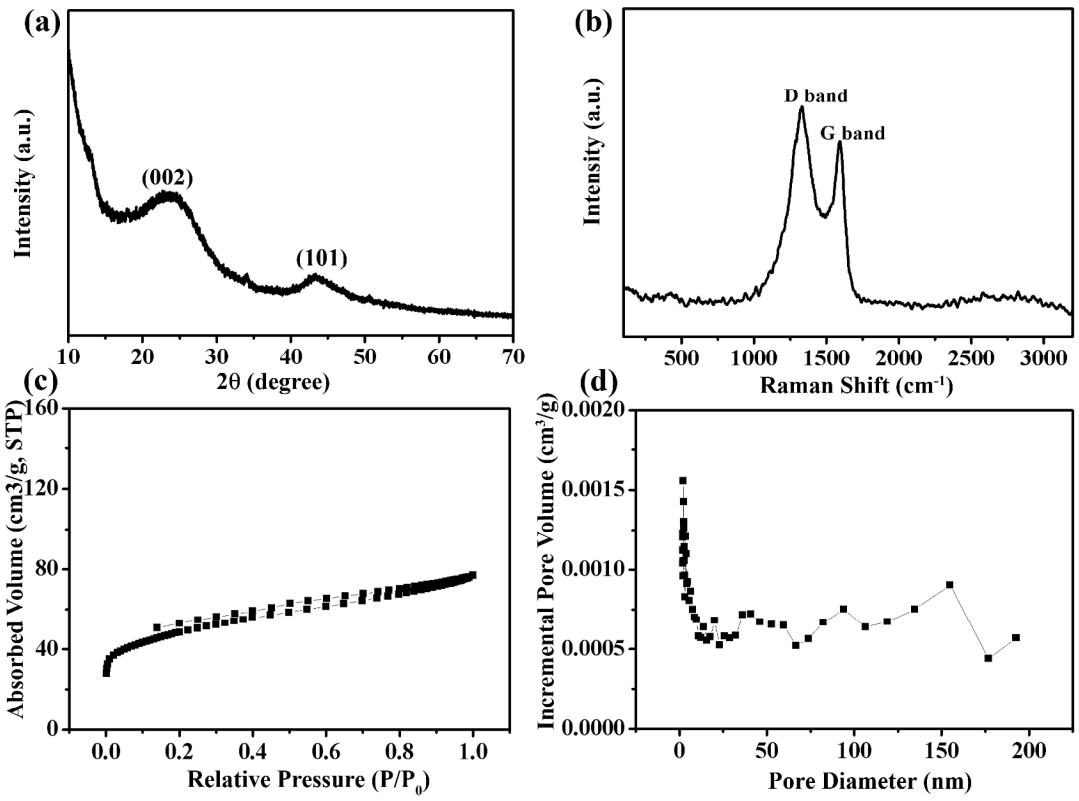

Figure 3. (a) XRD pattern and (b) Raman spectrum of the carbonized leaf. (c) N_2 adsorption-desorption isothermal curve and (d) the corresponding pore size distribution of the carbonized leaf.

To study the sodium ion storage properties, carbonized leaf is directly used as the electrodes in coin cells without using any binders, carbon additives or current

collectors. Figure 4a shows the first five potential profiles of the discharge/charge process, where a long potential plateau occurs near 0 V and a slope appears in the range of 0.2 V to 1.2 V. According to previous studies[30], the sloping region corresponds to the insertion of sodium ion into the short-range domains of ordered graphic lattice, with a value of 215.0 mAh/g, while the capacity from the plateau of 264.2 mAh/g is related to those "adsorption of sodium ions" at the defect sites and nanovoids. Overall, the specific capacity is 358.6 mAh/g for the first charge process and 479.2 mAh/g for the first discharge process, resulting an initial Coulombic efficiency as high as 74.8%. This value stabilized at about 100% from the second cycle on. Furthermore, the carbonized leaf maintains a high charge capacity of 360 mAh/g after 5 cycles at 10 mA/g. This excellent performance mainly results from the unique pore structure of the carbonized leaf, where the macropores are fully used but with limited SEI formation. The rate performance of the carbonized leaf is then studied, as shown in Figure 4b. The specific capacity can reach 320 mAh/g when the current intensity increases to 20 mA/g and has a value of 270 mAh/g at 40 mA/g. Furthermore, the carbonized leaf shows stable cycling performance, which delivered high capacity retention over 200 cycles (90%, Figure 4c). To study how the anisotropic surfaces affect the SIB performance, carbonized leaf was reversed as the electrode, where the upper surface faces to Na metal and back surface as the current collector. Interestingly, the first charge and discharge capacity dropped from 358.6 and 479.2 mAh/g to 246.2 and 325.1 mAh/g, respectively (Figure 4d), although the initial Coulombic efficiency remains roughly the same (74.8% to 75.7%). This reduced capacity may result from difficult sodium ion and electrolyte intrusion through the dense and thick upper surface layer.

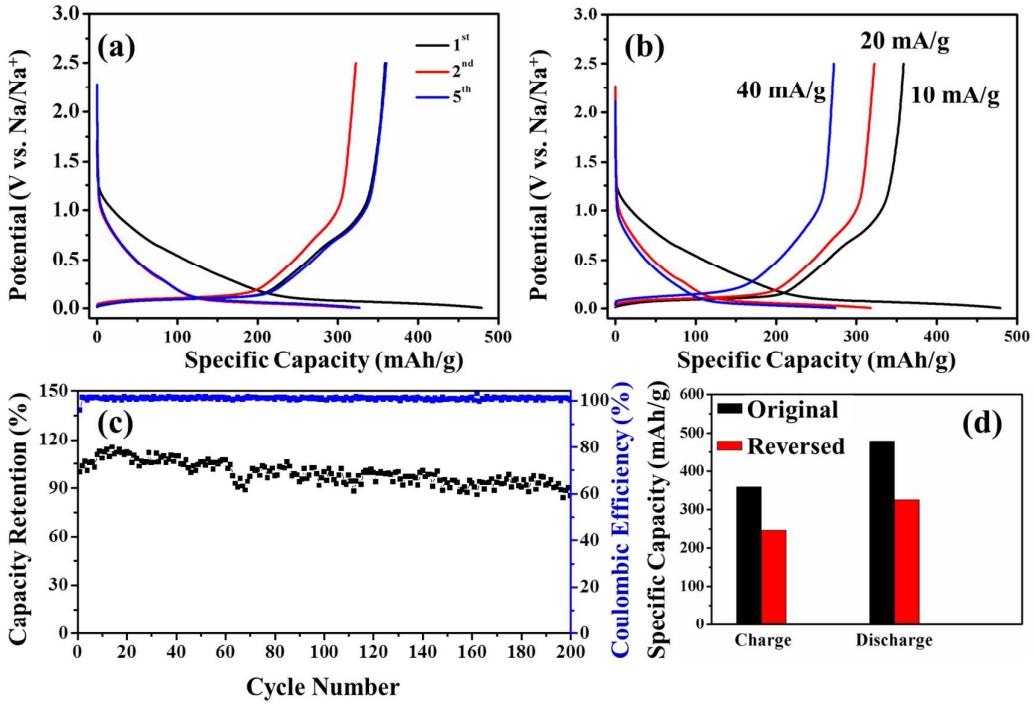

Figure 4. Electrochemical performance of the carbonized leaf anode for SIBs. (a) The first five charge/discharge curves. (b) Charge/discharge curves at the current densities of 10 mA/g, 20 mA/g and 40 mA/g. (c) The capacity retention and Coulombic efficiency over 200 cycles. (d) Comparison of carbonized leaves with different configurations in charge and discharge capacities.

The thin and flat structure of the carbonized leaf is suitable for scalable fabrication of electrode for the SIBs. By simply stacking the leaves together before the carbonization process, a continuous carbon membrane can be obtained (Figure 5a). These leaves are mostly welded together, as shown in the red box in Figure 5b, where a continuous interface was found. From the magnified SEM image of a welded leaf (Figure 5c), no clear interface is observed between two carbonized leaves, indicating most of the parts are indeed welded together. For the welding mechanism, several steps may be involved. First, organic components in leaves, such as cellulose,

hemicellulose and lignin were decomposed and small organic clusters were formed during the pyrolysis of leaves. Second, these clusters in the interface area between the two leaves would mix together to grow a uniform intermediate due to the molecules diffusion. Lastly, the intermediate in the interface would be carbonized at high temperature, which led to the formation of welded carbon product. With this method, a 3 cm by 3 cm carbon membrane was fabricated (Figure 5d). The conductivity of carbonized leaves was measured (Figure 5e). Based on the area of 1 cm by 1 cm and the thickness of 60 μm, the obtained conductivity is 1259 $S.m^{-1}$. With the effective welding by carbonization as shown in Figure 5b, the conductivity of two leaves welded together by carbonization is 710 $S.m^{-1}$ based on resistance measurement shown in Figure 5e. Note that thickness of the two leaves welded together is 120 μm. We also compare the conductivity of welded leaves with that of carbonized leaves by physical contact (Figure S6). As the anode, the welded leaves delivered a specific capacity of around 210 mAh/g (Figure S7), which is lower than a single carbonized leaf for the longer ionic diffusion path. The membrane made of leaves welded together by carbonization with a high electrical conductivity and good electrochemical performance show great promise as a low-cost, scalable SIB anode.

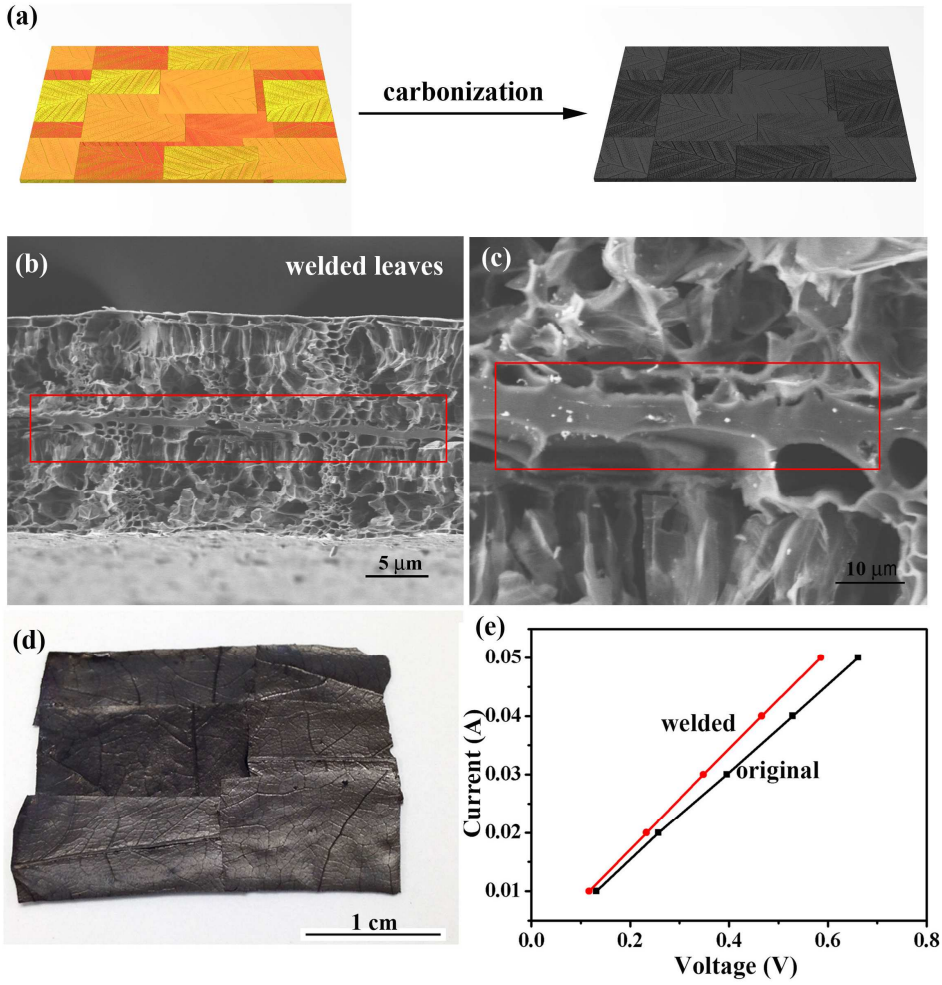

Figure 5. (a) Schematic of electrode membrane made of leaves welded together by carbonization. (b, c) SEM image of two leaves welded together by carbonization with an excellent contact, denoted by the red box. (d) A 3cm by 3 cm electrodes made of carbonized leaves which are welded together. (e) I-V measurement of a carbonized leaf (original) and a stack of two leaves welded together by carbonization.

CONCLUSION

In conclusion, we have synthesized freestanding carbon membranes from abundant natural leaves by a simple one-step carbonization process. The unique pore structure of the carbonized leaf makes it an ideal candidate for the anode of SIBs, which shows

a specific capacity of 360 mAh/g, a high initial Coulombic efficiency of nearly 75% and a stable cycling life. Moreover, the thin and flat structure of the leaves makes it easy to fabricate a large-area carbon membrane with low contact resistance by simply stacking multiple leaves together before the carbonization process. The excellent electrochemical performance and easily scalable fabrication method of these carbonized leaves make them promising in large-scale stationary energy storage.

ACKNOWLEDGMENTS

This work is funded by Energy Research Frontier Center (EFRC) funded by DOE, office of science, BES under award #DESC0001160. We would like thanks Dr. Sz-chian Liou for his kind help in TEM analysis. The Maryland Nanocenter and its Nisplab are also greatly acknowledged.

REFERENCES

(1). Yabuuchi, N.; Kubota, K.; Dahbi, M.; Komaba, S., Research Development on Sodium-ion Batteries. *Chem. Rev.* **2014,** *114*, 11636-11682.

(2). Kim, Y.; Ha, K.-H.; Oh, S. M.; Lee, K. T., High-capacity Anode Materials for Sodium-ion Batteries. *Chem. Eur. J.* **2014,** *20*, 11980-11992.

(3). Palomares, V.; Serras, P.; Villaluenga, I.; Hueso, K. B.; Carretero-González, J.; Rojo, T., Na-ion Batteries, Recent Advances and Present Challenges to Become Low Cost Energy Storage Systems. *Energ. & Environ. Sci.* **2012,** *5*, 5884-5901.

(4). Pan, H.; Hu, Y.-S.; Chen, L., Room-temperature Stationary Sodium-ion Batteries for Large-scale Electric Energy Storage. *Energ. & Environ. Sci.* **2013,** *6*, 2338-2360.

(5). Wang, L. P.; Yu, L.; Wang, X.; Srinivasan, M.; Xu, Z. J., Recent Developments in Electrode Materials for Sodium-ion Batteries. *J. Mater. Chem. A* **2015,** *3*,

9353-9378.

(6). Slater, M. D.; Kim, D.; Lee, E.; Johnson, C. S., Sodium-ion Batteries. *Adv. Funct. Mater.* **2013,** *23*, 947-958.

(7). Pasta, M.; Wessells, C. D.; Liu, N.; Nelson, J.; McDowell, M. T.; Huggins, R. A.; Toney, M. F.; Cui, Y., Full Open-framework Batteries for Stationary Energy Storage. *Nat. Commun.* **2014,** *5*, 3007.

(8). Ma, Z. H.; Wang, Y. S.; Sun, C. W.; Alonso, J. A.; Fernández-Díaz M. T.; Chen, L. Q., Experimental Visualization of the Diffusion Pathway of Sodium Ions in the $Na_3[Ti_2P_2O_{10}F]$ Anode for Sodium-ion Battery. *Sci. Rep.* **2015**, *4*, 7231.

(9). Kim, S.W.; Seo, D.H.; Ma, X.; Ceder, G.; Kang, K., Electrode Materials for Rechargeable Sodium-ion Batteries: Potential Alternatives to Current Lithium-ion Batteries. *Adv. Energ. Mater.* **2012,** *2*, 710-721.

(10). Fang, Y.; Xiao, L.; Qian, J.; Ai, X.; Yang, H.; Cao, Y., Mesoporous Amorphous $FePO_4$ Nanospheres as High-performance Cathode Material for Sodium-ion Batteries. *Nano Lett.* **2014,** *14*, 3539-3543.

(11). Wang, L.; Song, J.; Qiao, R.; Wray, L. A.; Hossain, M. A.; Chuang, Y. D.; Yang, W.; Lu, Y.; Evans, D.; Lee, J. J.; Vail, S.; Zhao, X.; Nishijima, M.; Kakimoto, S.; Goodenough, J. B., Rhombohedral Prussian White as Cathode for Rechargeable Sodium-ion Batteries. *J. Am. Chem. Soc.* **2015,** *137*, 2548-2554.

(12). Moradi, M.; Li, Z.; Qi, J.; Xing, W.; Xiang, K.; Chiang, Y. M.; Belcher, A. M., Improving the Capacity of Sodium Ion Battery Using a Virus-templated Nanostructured Composite Cathode. *Nano Lett.* **2015,** *15*, 2917-2921.

(13). Wang, S.; Wang, L.; Zhu, Z.; Hu, Z.; Zhao, Q.; Chen, J., All Oganic Sodium-ion Batteries with $Na_4C_8H_2O_6$. *Angew. Chem. Int. Ed.* **2014,** *53*, 5892-5896.

(14). Xiang, X.; Zhang, K.; Chen, J. Recent Advances and Prospects of Cathode Materials for Sodium-ion Batteries. *Adv. Mater.* **2015**, *27*, 5343-5364.

(15). Stevens, D.; Dahn, J. The Mechanisms of Lithium and Sodium Insertion in Carbon Materials. *J. Electrochem. Soc.* **2001**, *148*, A803-811.

(16). Kim, Y.; Park, Y.; Choi, A.; Choi, N.-S.; Kim, J.; Lee, J.; Ryu, J. H.; Oh, S. M.; Lee, K. T., An Amorphous Red Phosphorus/Carbon Composite as a Promising Anode Material for Sodium Ion Batteries. *Adv. Mater.* **2013,** *25*, 3045-3049.

(17). Xu, J.; Wang, M.; Wickramaratne, N. P.; Jaroniec, M.; Dou, S.; Dai, L., High-performance Sodium Ion Batteries Based on a 3D Anode from Nitrogen-doped Graphene Foams. *Adv. Mater.* **2015,** *27*, 2042-2048.

(18). David, L.; Bhandavat, R.; Singh, G., MoS_2/Graphene Composite Paper for Sodium-ion Battery Electrodes. *ACS Nano* **2014,** *8*, 1759-1770.

(19). He, G.; Li, L.; Manthiram, A., VO_2/rGO Nanorods as a Potential Anode for Sodium- and Lithium-ion Batteries. *J. Mater. Chem. A* **2015,** *3*, 14750-14758.

(20). Matsuo, Y.; Ueda, K., Pyrolytic Carbon from Graphite Oxide as a Negative Electrode of Sodium-ion Battery. *J. Power Sources* **2014,** *263*, 158-162.

(21). Prabakar, S. J. R.; Jeong, J.; Pyo, M., Nanoporous Hard Carbon Anodes for Improved Electrochemical Performance in Sodium Ion Batteries. *Electrochim. Acta* **2015,** *161*, 23-31.

(22). Komaba, S.; Murata, W.; Ishikawa, T.; Yabuuchi, N.; Ozeki, T.; Nakayama, T.;

Ogata, A.; Gotoh, K.; Fujiwara, K., Electrochemical Na Insertion and Solid Electrolyte Interphase for Hard-carbon Electrodes and Application to Na-ion Batteries. *Adv. Funct. Mater.* **2011,** *21*, 3859-3867.

(23). Bommier, C.; Luo, W.; Gao, W.Y.; Greaney, A.; Ma, S.; Ji, X., Predicting Capacity of Hard Carbon Anodes in Sodium-ion Batteries Using Porosity Measurements. *Carbon* **2014,** *76*, 165-174.

(24). Li, Y. M.; Mu, L. Q.; Hu, Y. S.; Li, H.; Chen, L. Q.; Huang, X. J., Pitch-derived Amorphous Carbon as High Performance Anode for Sodium-ion Batteries. *Energ. Storage Mater.* **2015**, *doi: 10.1016/j.ensm.2015.10.003*

(25). Zhang, L.; Liu, Z.; Cui, G.; Chen, L. Biomass-derived Materials for Electrochemical Energy Storages. *Prog. Polym. Sci.* **2015,** *43*, 136-164.

(26). Zhu, H.; Jia, Z.; Chen, Y.; Weadock, N.; Wan, J.; Vaaland, O.; Han, X.; Li, T.; Hu, L., Tin Anode for Sodium-ion Batteries Using Natural Wood Fiber as a Mechanical Buffer and Electrolyte Reservoir. *Nano Lett.* **2013,** *13*, 3093-3100.

(27). Wang, H.; Hu, P.; Yang, J.; Gong, G.; Guo, L.; Chen, X., Renewable-juglone-based High-performance Sodium-ion Batteries. *Adv. Mater.* **2015,** *27* (14), 2348-2354.

(28). Cao, Y. L.; Xiao, L. F.; Sushko, M. L.; Wang, W.; Schwenzer, B.; Xiao, J.; Nie, Z. M. Saraf, L. V.; Yang, Z. G.; Liu, J., Sodium Ion Insertion in Hollow Carbon Nanowires for Battery Applications. *Nano Lett.* **2012**, *12*, 3783-3787.

(29). Komaba, S.; Murata, W.; Ishikawa, T.; Yabuuchi, N.; Ozeki, T.; Nakayama, T.; Ogata, A.; Gotoh, K.; Fujiwara, K., Electrochemical Na Insertion and Solid

Electrolyte Interphase for Hard-carbon Electrodes and Application to Na-ion Batteries. *Adv. Funct. Mater.* **2011**, *21*, 3859-3867.

(30). Lotfabad, E. M.; Kalisvaart, P.; Kohandehghan, A.; Karpuzovc, D.; Mitlin, D. Origin of Non-SEI Related Coulombic Efficiency Loss in Carbons Tested Against Na and Li. *J. Mater. Chem. A* **2014**, *2*, 19685-19695.

(31). Raccichini,R.; Varzi,A.; Passerini, S.; Scrosati, B. The Role of Graphene in Electrochemical Energy Storage. *Science* **2015**, *14*, 271-279.

(32). Wang, Z. H.; Qie, L.; Yuan, L. X.; Zhang, W. X.; Hu, X. L.; Huang, Y. H., Functionalized N-doped Interconnected Carbon Nanofibers as an Anode Material for Sodium-ion Storage with Excellent Performance. *Carbon* **2013**, *55*, 328-334.

(33). Wang, C. S.; Wu, G. T;. Li, W. Z., Lithium Insertion in Ball-milled Graphite. *J. Power Sources* **1998**, *76*, 1-10.

(34). Alcantara, R.; Lavela, P.; Ortiz, G. F.; Tirado, J. L., Carbon Microspheres Obtained from Resorcinol-formaldehyde as High-capacity Electrodes for Sodium-ion Batteries. *Electrochem. Solid-State Lett.* **2005,** *8*, A222-A225.

(35). Li, Y. M.; Hu, Y. S.; Li, H.; Chen, L. Q.; Huang, X. J., A Superior Low-cost Amorphous Carbon Anode Made from Pitch and Lignin for Sodium-ion Batteries. *J. Mater. Chem. A* **2016**, *4*, 96-104.

(36). Li, Y.; Xu, S.; Wu, X.; Yu, J.; Wang, Y.; Hu, Y.S.; Li, H.; Chen, L.; Huang, X., Amorphous Monodispersed Hard Carbon Micro-spherules Derived from Biomass as a High Performance Negative Electrode Material for Sodium-ion Batteries. *J. Mater. Chem. A* **2015,** *3*, 71-77.

(37). Ding, J.; Wang, H.; Li, Z.; Kohandehghan, A.; Cui, K.; Xu, Z.; Zahiri, B.; Tan, X.; Lotfabad, E. M.; Olsen, B. C.; Mitlin, D., Carbon Nanosheet Frameworks Derived from Peat Moss as High Performance Sodium Ion Battery Anodes. *ACS Nano* **2013,** *7*, 11004-11015.

(38). Lotfabad, E. M.; Ding, J.; Cui, K.; Kohandehghan, A.; Kalisvaart, W. P.; Hazelton, M.; Mitlin, D., High-density Sodium and Lithium Ion Battery Anodes from Banana Peels. *ACS Nano* **2014,** *8*, 7115-7129.

(39). Luo, W.; Schardt, J.; Bommier, C.; Wang, B.; Razink, J.; Simonsen, J.; Ji, X., Carbon Nanofibers Derived from Cellulose Nanofibers as a Long-life Anode Material for Rechargeable Sodium-ion Batteries. *J. Mater. Chem. A* **2013,** *1*, 10662-10666.

(40). Hou, J.; Cao, C.; Idrees, F.; Ma, X., Hierarchical Porous Nitrogen-doped Carbon Nanosheets Derived from Silk for Ultrahigh-capacity Battery Anodes and Supercapacitors. *ACS Nano* **2015**, *9*, 2556-2564.

(41). Yun, Y.; Park, K.; Lee, B.; Cho, S.; Park, Y.; Hong, S.; Kim, B.; Gwon, H.; Kim, H.; , Lee, S.; Park, Y.; Jin, H. Kang, K., Sodium-ion Storage in Pyroprotein-based Carbon Nanoplates. *Adv. Mater.* **2015**, *27*, 6914-6921.

(42). Hong, K. L.; Qie, L.; Zeng, R.; Yi, Z. Q.; Zhang, W.; Wang, D.; Yin, W.; Wu, C.; Fan, Q. J.; Zhang, W. X.; Huang, Y. H., Biomass Derived Hard Carbon Used as a High Performance Anode Material for Sodium Ion Batteries. *J. Mater. Chem. A* **2014,** *2*, 12733-12738.

(43). Ha, D. H.; Islam, M. A.; Robinson, R. D., Binder-free and Carbon-free Nanoparticle Batteries: a Method for Nanoparticle Electrodes without Polymeric

Binders or Carbon black. *Nano Lett.* **2012,** *12*, 5122-5130.

(44). Zhou, G.; Zhao, Y.; Zu, C.; Manthiram, A., Free-standing TiO_2 Nanowire-embedded Graphene Hybrid Membrane for Advanced Li/Dissolved Polysulfide Batteries. *Nano Energy* **2015,** *12*, 240-249.

(45). Wang, C.; Wang, X.; Yang, Y.; Kushima, A.; Chen, J.; Huang, Y.; Li, J., Slurryless Li_2S/Reduced Graphene Oxide Cathode Paper for High-performance Lithium Sulfur Battery. *Nano Lett.* **2015,** *15*, 1796-1802.

(46). Ding, Y. L.; Wen, Y.; van Aken, P. A.; Maier, J.; Yu, Y., Rapid and Up-scalable Fabrication of Free-standing Metal Oxide Nanosheets for High-performance Lithium Storage. *Small* **2015,** *11*, 2011-2018.

(47). Sariyildiz, T.; Anderson, J. M., Variation in the Chemical Composition of Green Leaves and Leaf Litters from Three Deciduous Tree Species Growing on Different Soil Types. *Forest Ecol. Manag.* **2005,** *210*, 303-319.

(48). Chung, S.-H.; Manthiram, A., A Natural Carbonized Leaf as Polysulfide Diffusion Inhibitor for High-performance Lithium-sulfur Battery Cells. *Chem. Sus. Chem.* **2014,** *7*, 1655-1661.

(49). Wang, S. T.; Ying, Z.; Xia, F.; Xi, J. M.; Wang, N.; Feng, L.; Jiang, L., The Preparation of a Superhydrophilic Carbon Film from a Superhydrophobic Lotus Leaf. *Carbon* **2006,** *44*, 1848-1850.

(50). Han, S.-W.; Jung, D.-W.; Jeong, J.-H.; Oh, E.-S., Effect of Pyrolysis Temperature on Carbon Obtained from Green Tea Biomass for Superior Lithium Ion Battery Anodes. *Chem. Eng. J.* **2014,** *254*, 597-604.

(51). Li, X.; Fan, T.; Zhou, H.; Chow, S.-K.; Zhang, W.; Zhang, D.; Guo, Q.; Ogawa, H., Enhanced Light-harvesting and Photocatalytic Properties in Morph-TiO_2 from Green-leaf Biotemplates. *Adv. Funct. Mater.* **2009,** *19*, 45-56.

(52). Zhou, H.; Guo, J.; Li, P.; Fan, T.; Zhang, D.; Ye, J., Leaf-architectured 3D Hierarchical Artificial Photosynthetic System of Perovskite Titanates Towards CO_2 Photoreduction Into Hydrocarbon Fuels. *Sci. Rep.* **2013,** *3*, 1667.

(53). Schnepp, Z.; Yang, W.; Antonietti, M.; Giordano, C., Biotemplating of Metal Carbide Microstructures: the Magnetic Leaf. *Angew. Chem. Int. Ed.* **2010,** *49*, 6564-6566.

(54). Hu, H.; Zhao, Z.; Wan, W.; Gogotsi, Y.; Qiu, J., Ultralight and Highly Compressible Graphene Aerogels. *Adv. Mater.* **2013,** *25*, 2219-2223.

(55). Bircan, S. Y.; Naruse, I.; Matsumoto, K.; Kitagawa, K., Production of Hydroxylapatite from Biowaste, Chicken Manure by Hydrothermal Process. *J. Sustain. Bioenerg. Sys.* **2013**, *3*, 74-78.

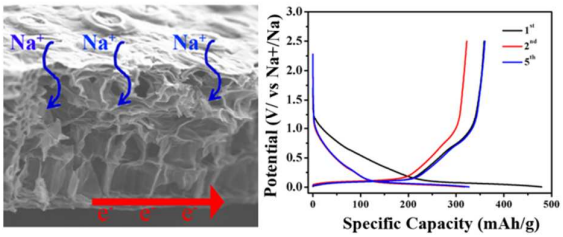

Table of Contents (TOC) graphic